

Pedro Guilherme da Cunha Leit o Dias Vaz

METHODS FOR HEMODYNAMIC PARAMETERS MEASUREMENT USING THE LASER SPECKLE EFFECT IN MACRO AND MICROCIRCULATION

PhD thesis in Biomedical Engineering, in co-supervision (co-tutelle) regime between the University of Coimbra (UC) — Portugal and the University of Angers (UA) — France, under the supervision of Dr. Jo o Manuel Rendeiro Cardoso (UC) and Professor Anne Humeau-Heurtier (UA), submitted to the Faculty of Sciences and Technology.

16 de Novembro 2016

Background

Introduction

Laser speckle is an interferometric effect that results from the interaction of coherent waves.

Applications on: Material characterization; Velocity estimation; Speech reconstruction;

Laser speckle imaging (LSI) is used for microcirculation assessment in highly vascularized tissues. The red blood cells movements produce variations in the speckle interference pattern.



Goals

Introduction

Macrocirculation

Determine if laser speckle can be used to assess macrocirculation parameters.

Which light wavelength produces better results.

Use the same processing method used for LSI in order to facilitate system integration.

Microcirculation

Study of the effect of static scatterers on the laser speckle contrast and correlation.

Characterization of laser speckle correlation as method to determine the static scatterers concentrations.

Contrast algorithm optimization study.

Speckle Contrast

Laser Speckle Imaging

Laser speckle contrast (K) is usually computed using the image standard deviation and/or image intensity mean.

$$K = \frac{\sigma_s}{\langle I \rangle} = \frac{\sqrt{\langle (I - \langle I \rangle)^2 \rangle}}{\langle I \rangle} .$$

The contrast can be related with the scatterers decorrelation time (τ) by:

$$K^2(T) = \frac{2\beta}{T} \int_0^T [(1 - \rho)^2 |g_{1d}(\tau)| + \rho]^2 \left(1 - \frac{\tau}{T}\right) d\tau$$

Velocity
distribution
model

Beta (β) is a correction factor that accounts for experimental imperfections.

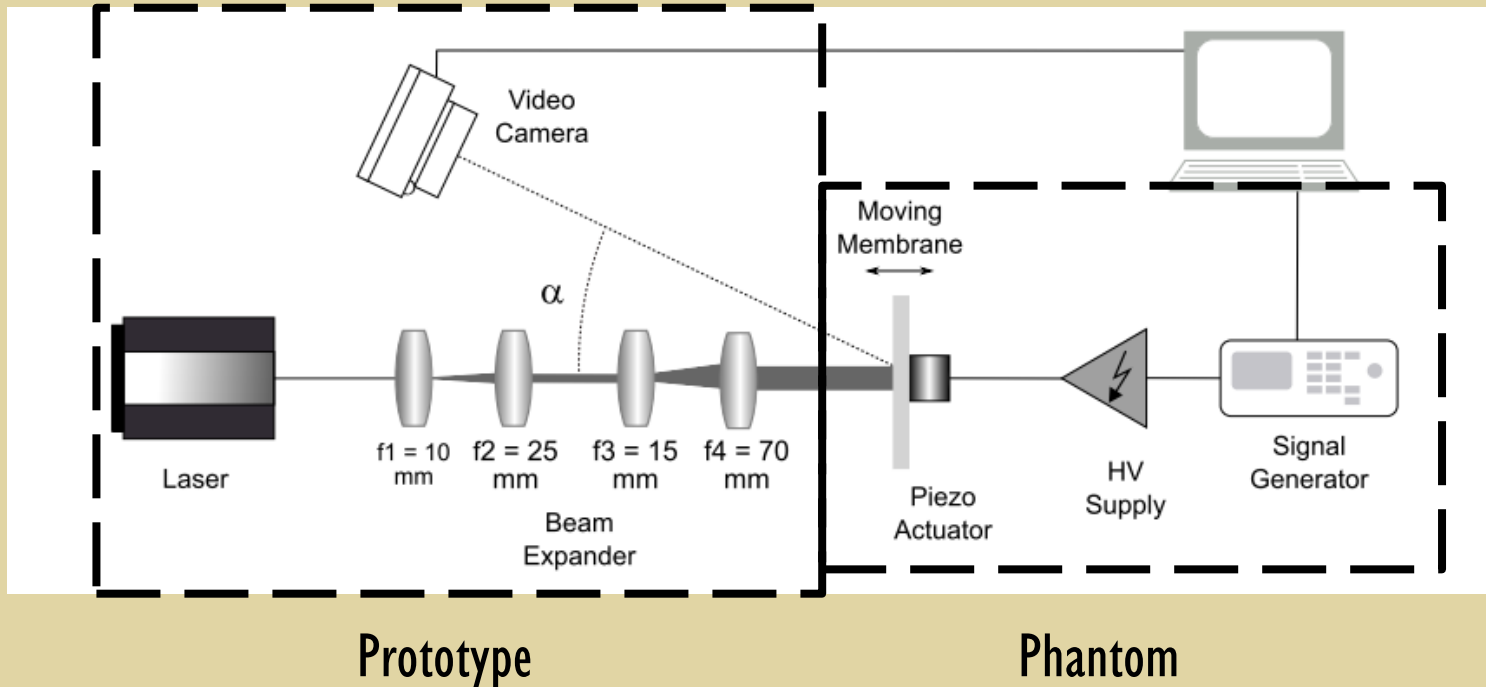
Rho (ρ) is a quantity that accounts for the presence of dynamic scatterers.

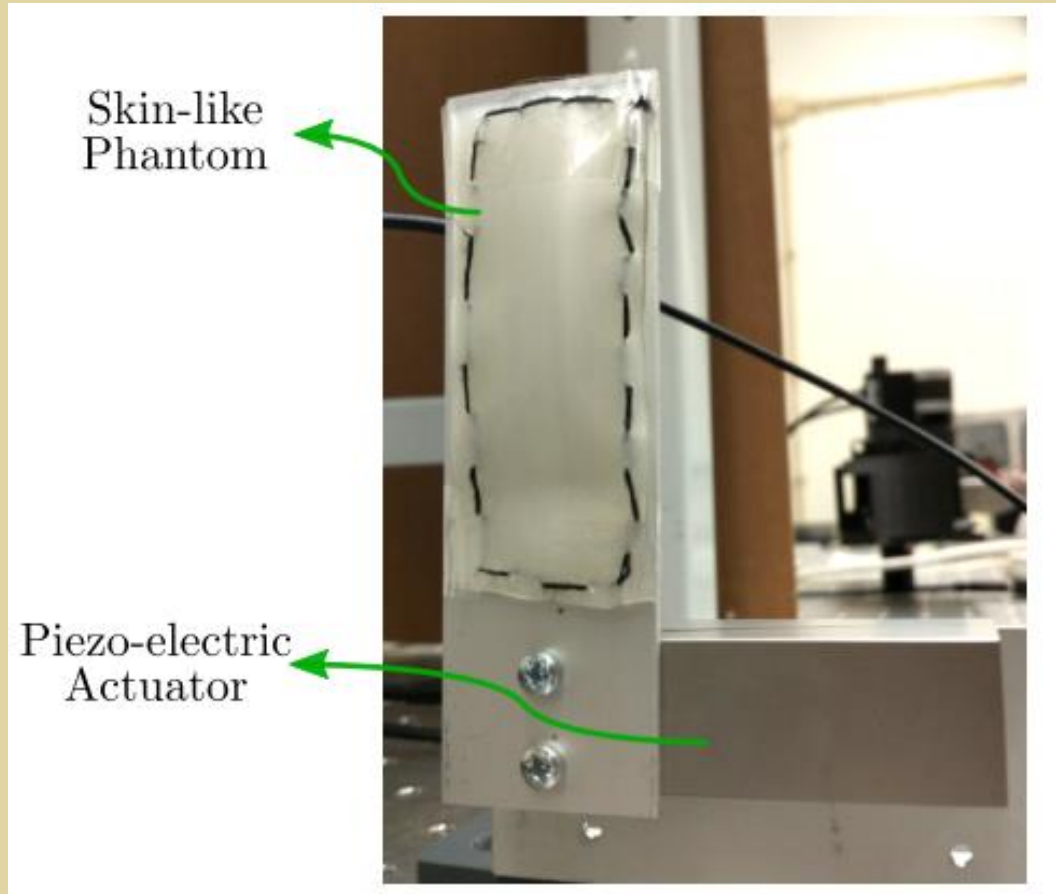
Experimental bench test

Macrocirculation methods

Determine which wavelength performs better to extract macrocirculation parameters.

Test based on an LSI prototype and a moving phantom:





Multi-Wavelength study - bench

Phantom movements:

Frequencies: 1, 1/2, 1/4 and 1/5 Hz.

Amplitudes: 2, 4, and 8 peak to peak voltage.

Signal processing

2D correlation coefficient between consecutive images.

Macrocirculation methods

Prototype specs:

Sources: Green - 532nm and 4.5mW.

Red - 635nm and 4.9mW.

Infra-red - 850nm and 3mW.

Phantom specs:

4 white translucent silicone membranes.

Area of 30mm x 60mm.

Connected to a piezoelectric actuator.

Transversal movement.

$$r = \frac{\sum_x \sum_y (A_{xy} - \bar{A})(B_{xy} - \bar{B})}{\sqrt{(\sum_x \sum_y (A_{xy} - \bar{A})^2)(\sum_x \sum_y (B_{xy} - \bar{B})^2)}}$$

Multi-Wavelength study – in vivo

Macrocirculation methods

2 Subjects: 27 years old female and 24 years old male.

Assessment of radial artery.

Lack of PPG synchronism.

Application of 2D-Correlation coefficient.

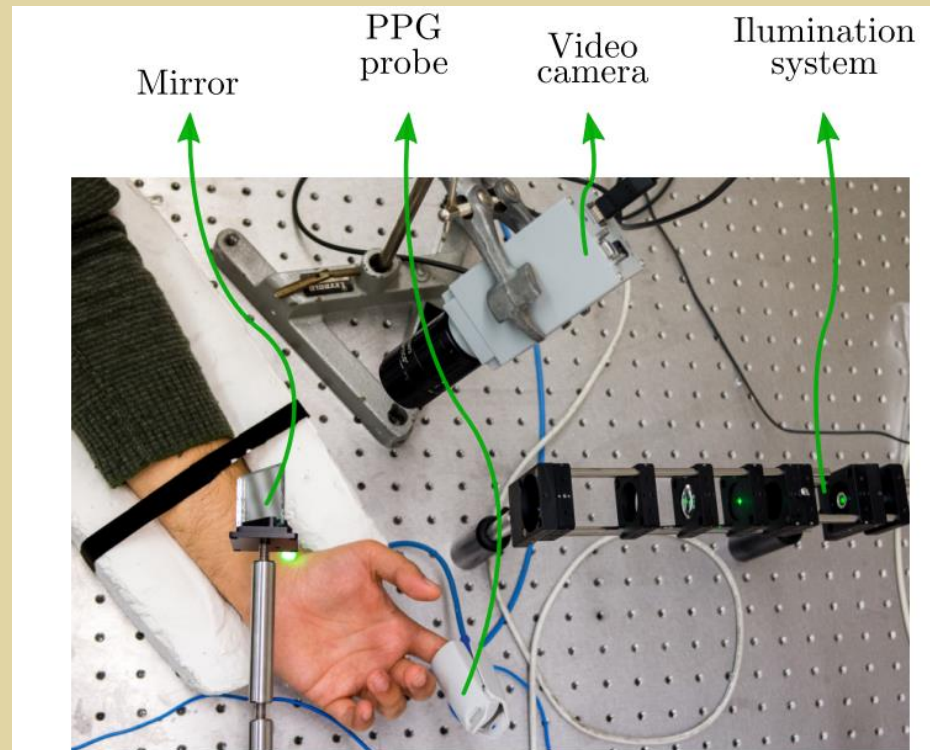


Figure 4.4: Photography of the *in vivo* acquisition scheme.

Pulse waveform extraction (PWE) study

Macrocirculation methods

Use of the most suitable laser light wavelength in 10 Healthy volunteers, 3 acquisitions per subject.

Signal processing:

Overall frame spatial contrast:

$$K = \frac{\sigma_s}{\langle I \rangle} = \frac{\sqrt{\langle (I - \langle I \rangle)^2 \rangle}}{\langle I \rangle} .$$

Evaluation metrics:

Heart rate determination using FFT.

Spectral similarity (SI)

$$C_{KP}(f) = \frac{|P_{KP}(f)|^2}{P_K(f)P_P(f)} ,$$

$$SI = \int_0^{10} C_{KP}(f) df .$$

Multi-wavelengths results - bench

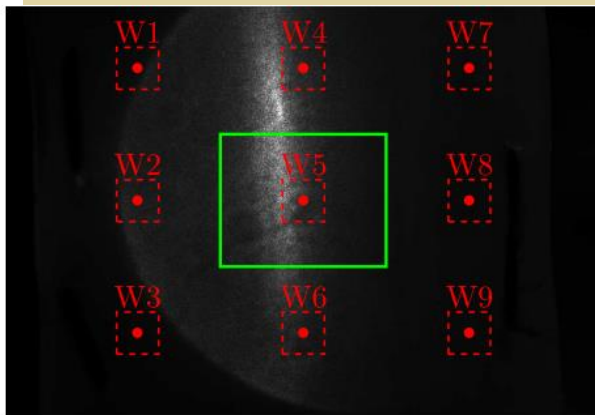
Macrocirculation results

Different light wavelengths show different speckle granularities and different blurring degrees.

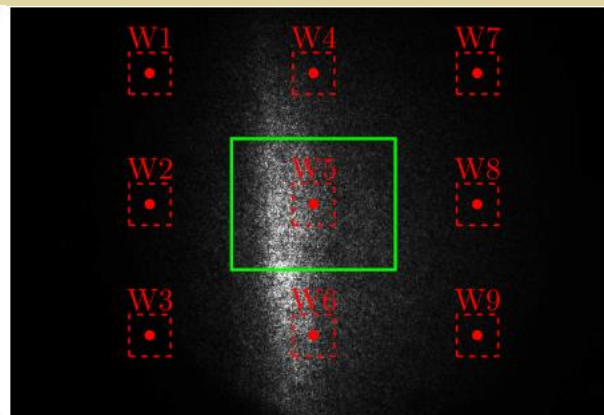
This differences occur because each wavelength has different skin penetrations.

Images of the silicone layer phantom.

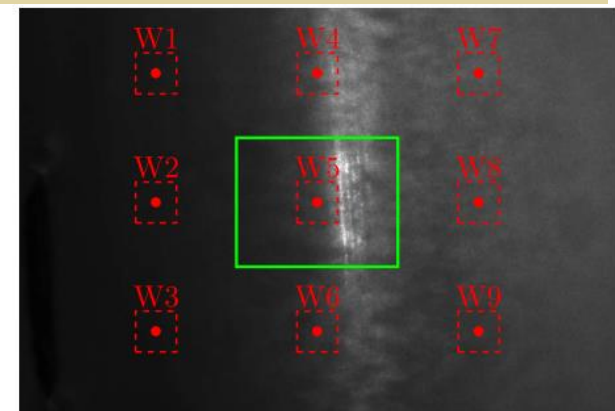
The infrared image is much more blurred than the other two cases.



(a) L_{532} - Green



(b) L_{635} - Red



(c) L_{850} - Infra-red

Multi-wavelengths results - bench

Macrocirculation results

Overall errors between 9% and 20%. No differences between the three wavelengths.

Lower errors for slow movements and better consistency for green wavelengths.

Good profile reconstruction.

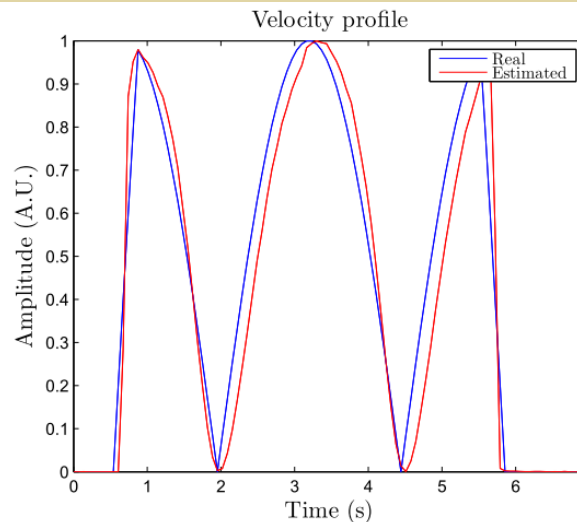


Figure 5.4: Plot of $1 - r'$ along time (red line) and absolute velocity of the phantom (blue line) of the movement with amplitude of $2V_{pp}$ and 5 seconds of period.

| | Period (s) | Amplitude (V_{pp}) | | |
|-----------|------------|------------------------|-------|-------|
| | | 2 | 4 | 8 |
| L_{532} | 1 | 20.68 | 11.87 | 19.31 |
| | 2 | 18.63 | 15.08 | 12.68 |
| | 3 | 15.55 | 9.92 | 9.52 |
| | 5 | 12.22 | 9.45 | 10.21 |
| L_{635} | 1 | 17.38 | 18.96 | 19.58 |
| | 2 | 20.83 | 21.68 | 24.91 |
| | 3 | 12.54 | 20.66 | 25.11 |
| | 5 | 10.31 | 16.78 | 26.64 |
| L_{850} | 1 | 16.27 | 14.78 | 13.26 |
| | 2 | 16.11 | 12.19 | 13.83 |
| | 3 | 20.42 | 13.97 | 9.02 |
| | 5 | 21.62 | 22.64 | 14.89 |

Multi-wavelengths results – in vivo

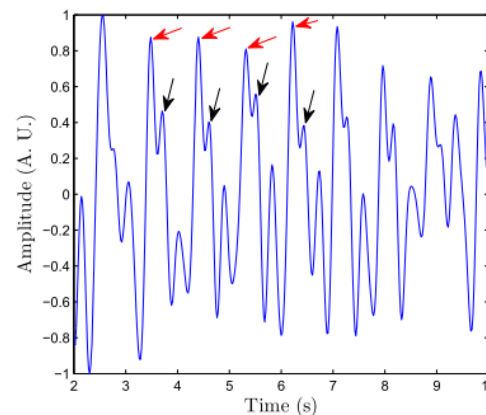
HR identification with errors less than 0,5 bpm for green laser and less than 1,3 bpm for red laser.

Infra-red laser showed poor results.

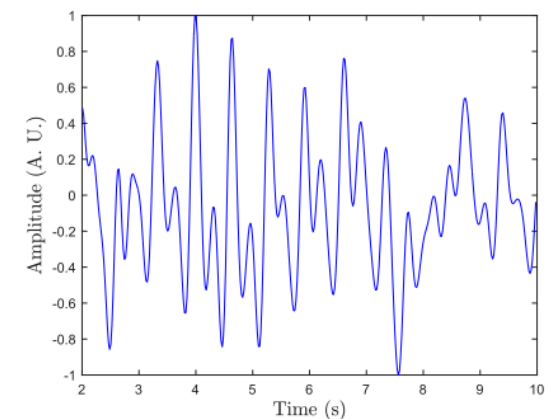
Graphical analysis show that green laser can reconstruct a more reliable pulse pressure wave.

Macrocirculation results

| | Data set | S1 | S2 | S3* | S4 | S5 | S6 | $g \epsilon_{rms}$ |
|-----------|--------------------|------|------|------|------|------|------|--------------------|
| L_{532} | Subject HR | 62.3 | 62.3 | 64.1 | 65.9 | 67.8 | 67.8 | |
| | No pre-process | 61.4 | 62.4 | 69.6 | 65.7 | 67.6 | 67.2 | 0.50 (2.28) |
| | Binarization | 61.5 | 61.9 | 69.5 | 65.7 | 67.4 | 67.4 | 0.48 (2.24) |
| | Hist. equal. | 61.4 | 62.3 | 69.6 | 65.7 | 67.6 | 67.2 | 0.50 (2.28) |
| | $d \epsilon_{rms}$ | 0.79 | 0.22 | 5.46 | 0.18 | 0.26 | 0.50 | |
| | Data set | S7 | S8 | S9 | S10 | S11 | S12 | $g \epsilon_{rms}$ |
| L_{635} | Effective HR | 64.1 | 65.9 | 67.7 | 82.4 | 89.7 | 60.4 | |
| | No pre-process | 66.4 | 66.0 | 68.7 | 82.4 | 88.6 | 59.6 | 1.15 |
| | Binarization | 66.7 | 65.6 | 68.7 | 82.5 | 88.5 | 59.6 | 1.26 |
| | Hist. equal. | 66.4 | 65.9 | 68.7 | 82.4 | 88.6 | 59.6 | 1.15 |
| | $d \epsilon_{rms}$ | 2.38 | 0.22 | 0.92 | 0.05 | 1.13 | 0.82 | |



(a) L_{532}



(b) L_{635}

Pulse waveform extraction results

Macrocirculation results

PPG data synchronized with the speckle data makes possible to compare both signals directly. In this test only the green laser was used because it presented the best results.

Similar waveforms for both PPG data and speckle contrast data.

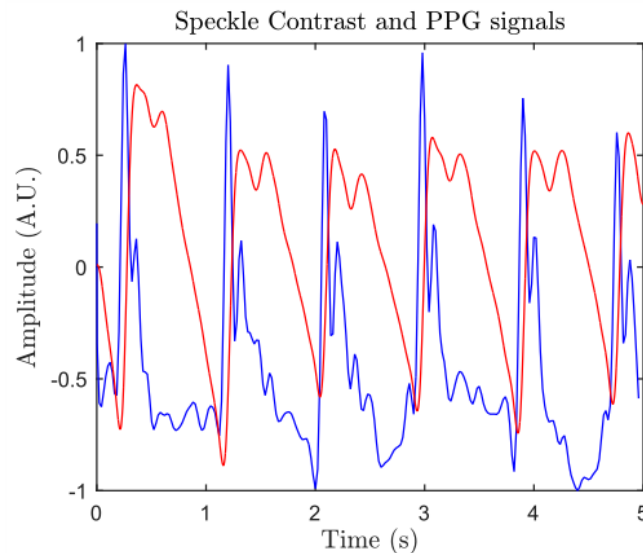
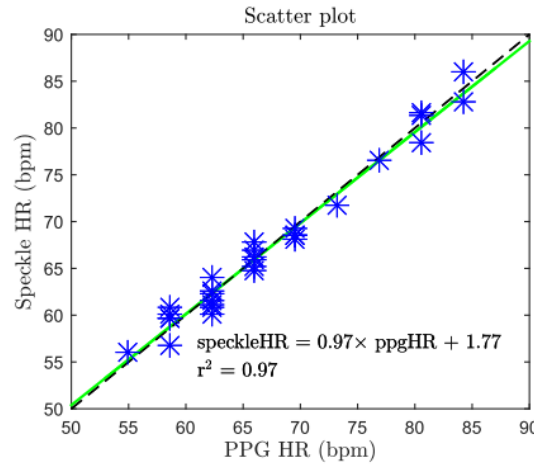


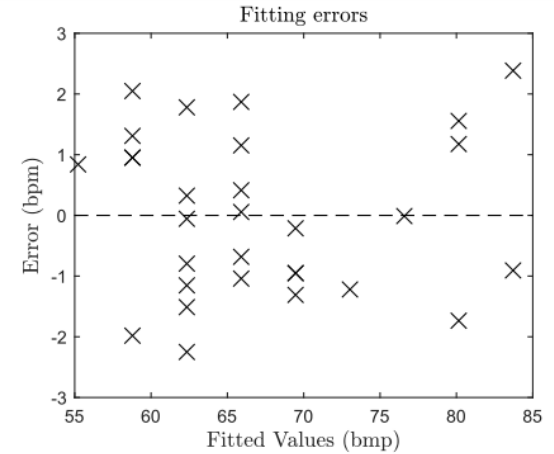
Figure 5.7: Temporal representation of PPG data (red line) and speckle contrast data (blue line).

HR determination error do not increase with the increasing Of its absolute value. Errors are always smaller than 3 bpm.

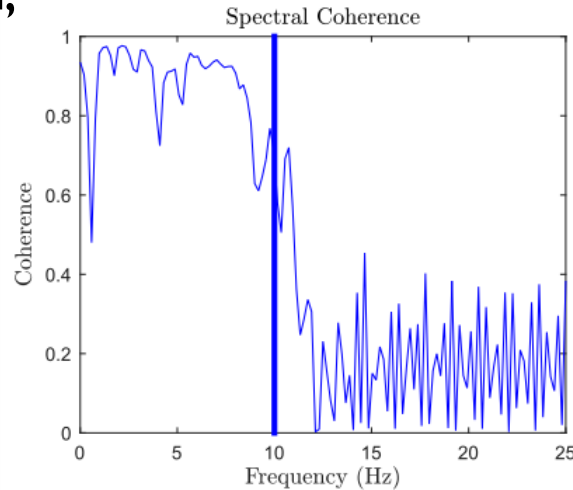
The mean SI is above 0.6 and, for a specific case reaches almost 0.9



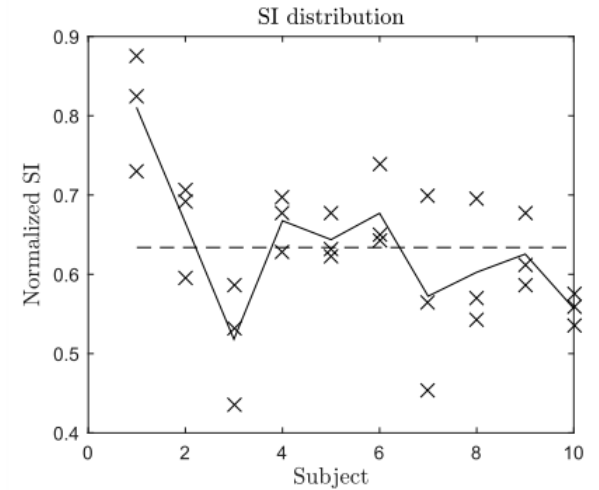
(a) Scatter plot



(b) Fitting errors



(a)



(b)

Microcirculation studies

During this test LSI data was recorded from a sample with different concentrations of static and dynamic characters.

Phantom composed by two phases:

Acrylic microchannel with 0.5mm depth,
and variable width (2 to 5 mm).

Silicone layers doped with
different concentrations of TiO_2 .

Dynamic scatterers simulated by milk
flowing through the channel.

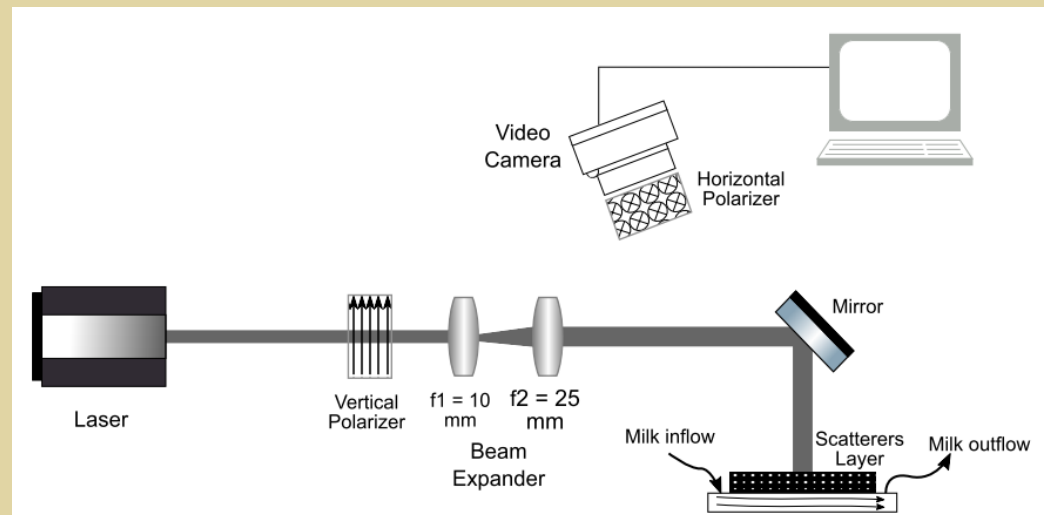


Figure 4.7: Optical scheme of the microcirculation bench set-up.

Phantom

Microcirculation methods

Complete phantom

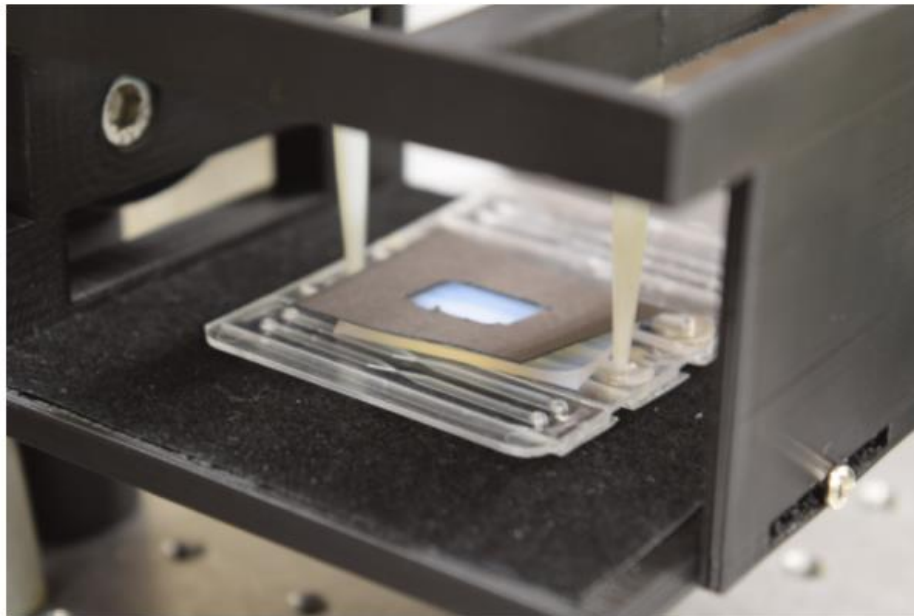


Figure 4.9: Lateral photography of the sample. The microchannel device is visible under the static scatterers layer. Two pipette tips are used to inject and remove the fluid.

Signal processing

Microcirculation methods

Speckle correlation was computed in small windows of 5x5 pixels (similar to contrast):

$$g_2(\Delta t) = \frac{\langle A \circ B \rangle_s}{\langle A \rangle_s \langle B \rangle_s},$$

Where $\langle \rangle$ represents the spatial average and “o” stands for the element by element multiplication.

The correlation is related with the scatterers concentrations by:

$$g_2(\Delta t) = 1 + \beta \left(\frac{\langle I_s \rangle}{\langle I_s \rangle + \langle I_d \rangle} \right)^2.$$

An increase of the static scatterers concentration results in an increase of the speckle correlation.

Contrast algorithm optimization study

Microcirculation methods

Algorithm optimization is a key factor when online applications are necessary, or large amount of data is analyzed.

4 Implementations were used in MATLAB:

Analytical Computation

Filtering implementation (imfilter)

Moving sum implementation (movsum)

Correlation implementation (conv2)

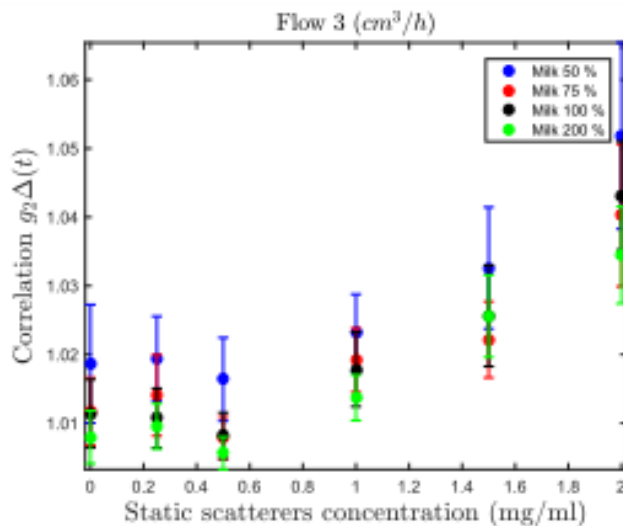
Speckle Correlation

Microcirculation results

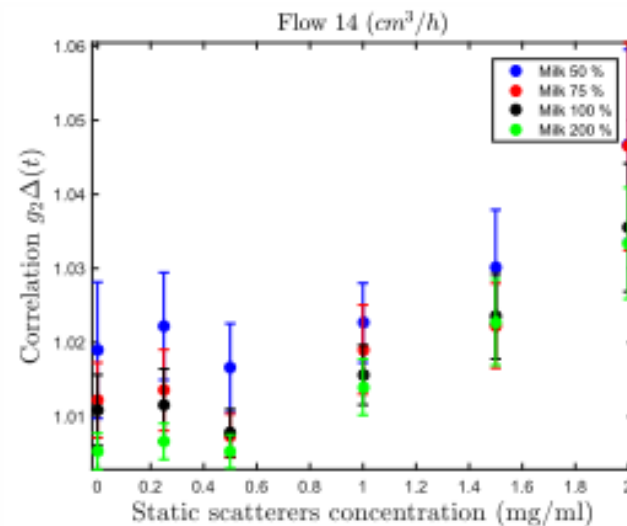
Visible increase of correlation when the static scatterers increase.

Visible decrease of the correlation with the increase of dynamic scatterers.

The error bars show that fluids with more dynamic scatterers produce laser speckle signals with higher reliability.



(c)

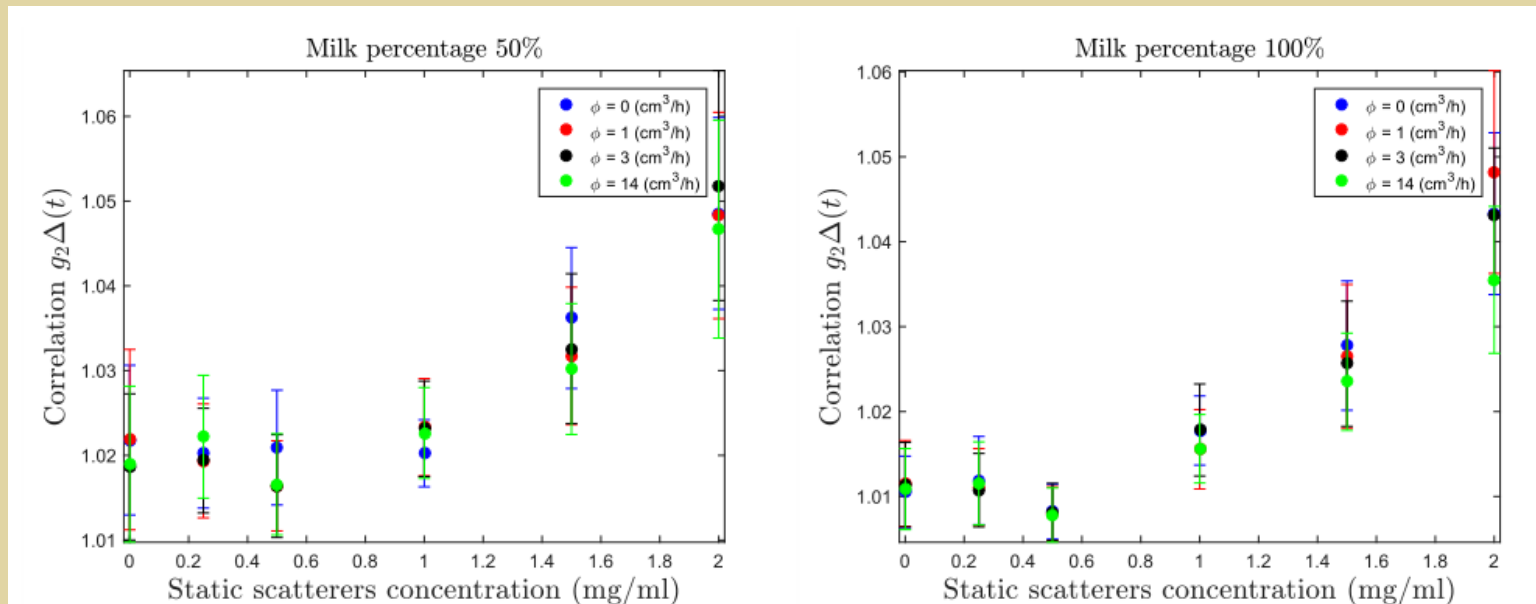


(d)

Speckle Correlation

Microcirculation results

The variations of fluid flow (ϕ) do not produce a relevant effect in the speckle correlation.

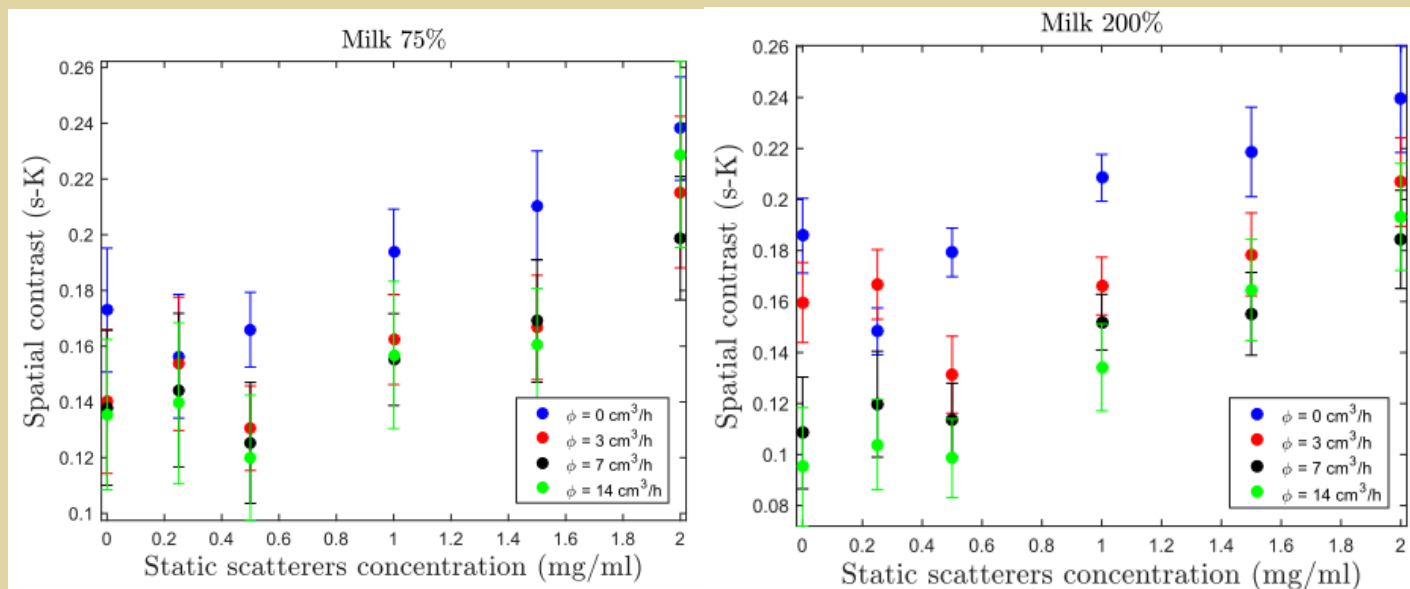


Speckle Contrast

Microcirculation results

Spatial contrast strongly influenced by variations in the static scatterers concentration.

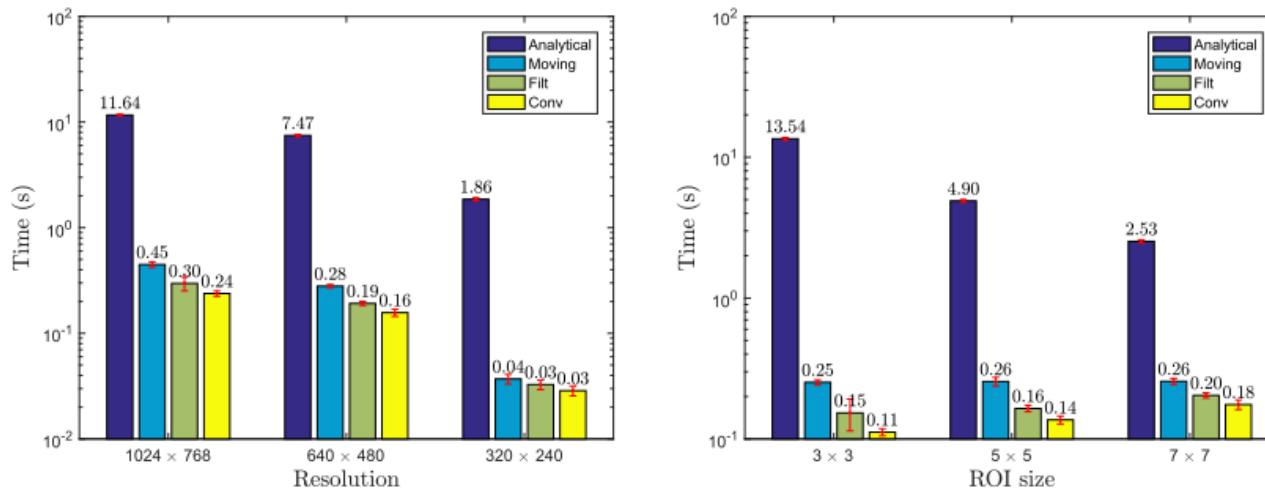
The contrast values are also sensitive to the changes in the fluid velocity which is the basis of the LSI theory.



Contrast algorithm optimization

Microcirculation results

The results show that the novel proposed implementation has achieved the best performance for all the tested cases.



(a) Computation time as function of the LS image resolution. (b) Computation time as function of the ROI size.

Figure 5.24: Analysis of the time required to process a single speckle image. The error bars represented in red correspond to the standard deviation.

Conclusions

Macrocirculation: LSI was used to extract the pulse pressure waveform with encouraging results. Shorter wavelengths have obtained the best results.

Microcirculation: Speckle correlation could be used to estimate the relation between dynamic and static scatterers. This metric is independent of the flow velocity which is the major conclusion of this study.

Limitations

Macrocirculation: The low frame rate of the video camera and the movement artifacts are a major problem of the application of this technique.

Microcirculation: The lack of quantification on the concentration of dynamic and static scatterers impedes this study to compute the ρ value. Also the phantom should be improved in order to be more homogenous.

Thank you.
pvaz@lei.fis.uc.pt

Biomedical Applications

Introduction

Laser speckle imaging (LSI) is used for microcirculation assessment in highly vascularized tissues.

The red blood cells movements produce variations in the speckle interference pattern. If these patterns are imaged by a system with finite exposure time ($T > 0$) the image became defocused.

Technique based on image contrast measurements.

Novel applications on low vascularized tissues (high concentration of static scatterers).

- The presence of static scatterers influence the speckle contrast values.
- Possibility to explore macrocirculation extraction parameters.

Microcirculation analysis

Laser Speckle Imaging

Speckle general equation relates contrast values with decorrelation times using the imaging system exposure time, β and ρ . The following equation corresponds to the evaluation of integral of slide 5 using a Lorentzian velocity distribution model.

$$x = T/\tau_c.$$

$$K(T)^2 = \beta \left[(1 - \rho)^2 \frac{e^{-2x} - 1 + 2x}{2x^2} + 4\rho(1 - \rho) \frac{e^{-x} - 1 + x}{x^2} + \rho^2 \right],$$

τ is posterior related with the scatterers velocity using the light wavelength:

$$V = \frac{\lambda}{2\pi \tau_c},$$

Contrast Algorithms

Laser Speckle Imaging

Speckle contrast is computed in small regions with or without overlapping.

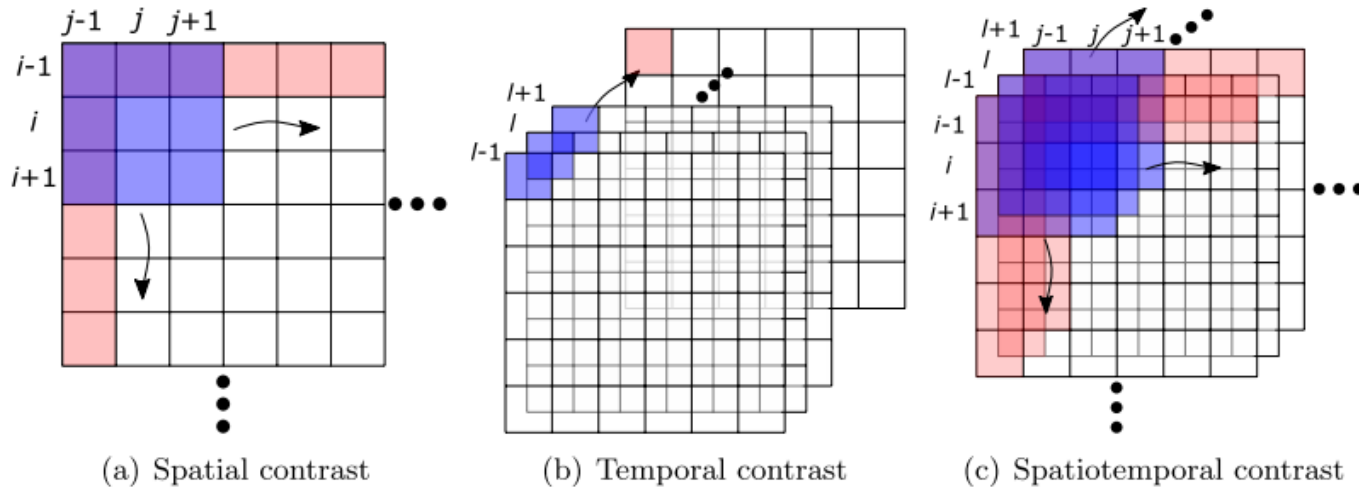


Figure 3.6: Illustration of the elements to compute contrast. The element is represented by blue squares. Pink squares represent the boundaries where the computation of contrast requires padding. Curved arrows were used to indicate the element displacement directions.

Macrocirculation

Methods

Advantages of using LSI to macrocirculation assessment:

- Truly non-contact method.

- Can be used to measure biomedical parameters at long distances.

- Possibility to extract joint features from macro and microcirculation parameters from the same data set.

Issues to be addressed:

- Determine the best light wavelengths for macrocirculation measurements.

- Sensitivity of LSI to macrocirculation processes.

Vibration frequency determination

Macrocirculation methods

Phantom movements:

Frequencies: 1, 2, 4 and 5 Hertz

Amplitudes: 0.5, 1, 2 and 4 Vpp

Movements applied to the phantom during all the experiments and correspondent peak velocity:

Table 4.2: Maximum skin-phantom displacements and maximum velocities according to the excitation signal parameters amplitude and frequency. The velocities are expressed in millimetres per second. Cells with - correspond to configurations not used in this work.

| Amplitude (V_{pp}) | Max. displacement (mm) | Frequency (Hz) | | | | | | | |
|---------------------------|---------------------------|----------------|------|------|------|------|------|------|--|
| | | 1/5 | 1/3 | 1/2 | 1 | 2 | 3 | 5 | |
| 0.5 | 0.05 | - | - | - | 0.15 | 0.29 | 0.44 | 0.60 | |
| 1 | 0.09 | 0.06 | 0.10 | 0.15 | 0.29 | 0.59 | 0.88 | 1.47 | |
| 2 | 0.19 | 0.12 | 0.20 | 0.29 | 0.59 | 1.17 | 1.76 | 2.93 | |
| 4 | 0.37 | 0.23 | 0.39 | 0.59 | 1.17 | 2.34 | 3.52 | 5.86 | |
| 6 | 0.56 | 0.35 | 0.59 | 0.88 | 1.76 | - | - | - | |
| 8 | 0.75 | 0.47 | 0.78 | 1.17 | 2.35 | - | - | - | |

Vibration frequency determination

Macrocirculation methods

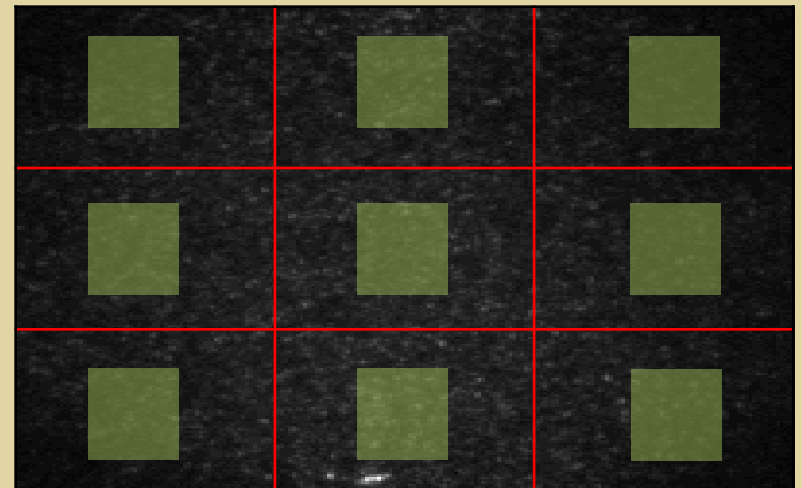
Power spectral density (PSD) of the pixels temporal evolution.

PSD computed in small image windows with different locations and sizes.

$$PSD_{(x,y)}(f_t) = \left| \sum_{t=1}^K I(x, y, t) \times e^{\frac{-i2\pi(t-1)(f_t-1)}{K}} \right|^2 ,$$

Sizes: 3x3, 9x9, 17x17, 81x81 pixels.

Locations: 9 zones - Green squares.



In vivo processing

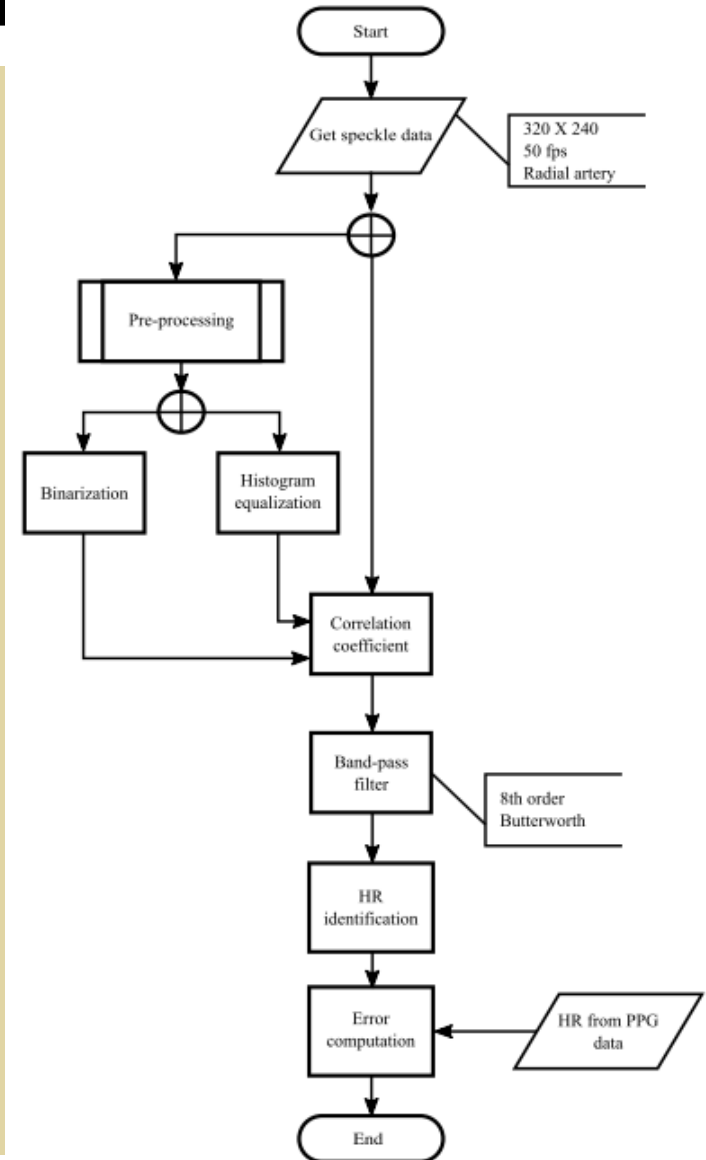
Application of the 2D-correlation coefficient.

Test of enhancement image processing techniques:

Binarization

Histogram equalization

Application of band-pass filter to improve signal reliability.

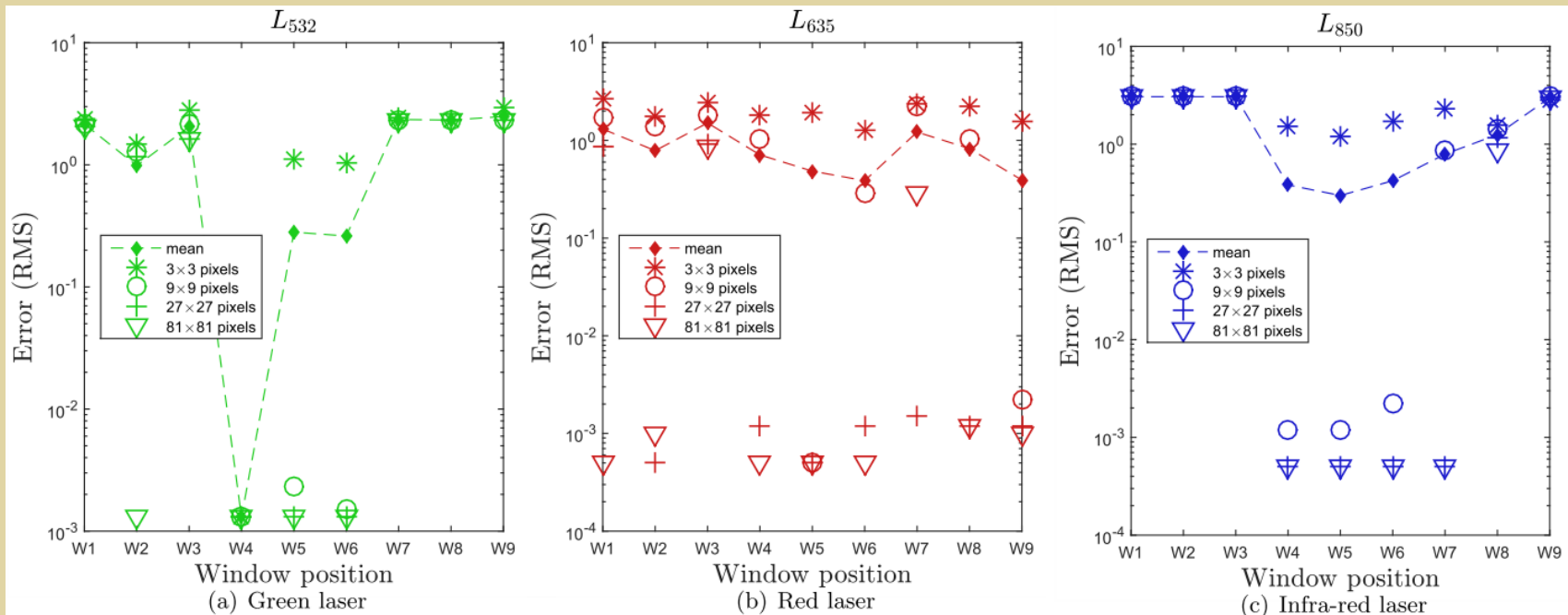


Vibration frequency determination

Macrocirculation results

Green light presents more heterogenous results because light dispersion is anisotropic.

All the light sources achieved errors in the order of 1.3 mHz to 0.5 mHz and for the larger windows (81x81 pixels).



Remarks

Macrocirculation results

Laser speckle can be used to record the pulse pressure waveform and extract macrocirculation parameters.

The green light proved to be better in extracting this information.

Both 2D correlation coefficient and overall contrast can be used to extract the pulse pressure waveform.

Issues:

Low camera sampling frequency compromise the extraction of the pulse waveform rapid features like the systolic peak or the dichotic notch. Low laser power decrease the global contrast of the images.

Experimental parameters

Microcirculation methods

6 layers with different static scatterers (TiO_2) concentrations have been produced:

Table 4.4: Scatterers concentration of the silicone layers.

| Layer | I | II | III | IV | V | VI |
|----------------------------------|---|------|-----|----|-----|----|
| Scatterers concentration (mg/ml) | 0 | 0.25 | 0.5 | 1 | 1.5 | 2 |

4 Different milk concentrations 50%, 75%, 100% and 200% (addition of powdered milk).

5 Different fluid flows:

Table 4.3: Relationship between the phantom inflow and the fluid velocity in the core of the wider segment.

| Case # | Flow (cm^3/h) | Core velocity (mm/s) |
|--------|---------------------------------|--|
| 0 | 0 | 0 |
| 1 | 1.5 | 0.26 |
| 2 | 3 | 0.53 |
| 3 | 7 | 1.25 |
| 4 | 14 | 2.50 |

Signal processing

Microcirculation methods

A value of mean correlation and standard deviation has been computed for each configuration.

Moreover, speckle contrast has been computed using the three main algorithms, spatial, temporal and spatiotemporal.

s-K element size 5x5 pixels.

t-K element size 1x1x15 pixels.

st-K element size 3x3x5 pixels.

Again, a value of mean and standard deviation was computed for each configuration.

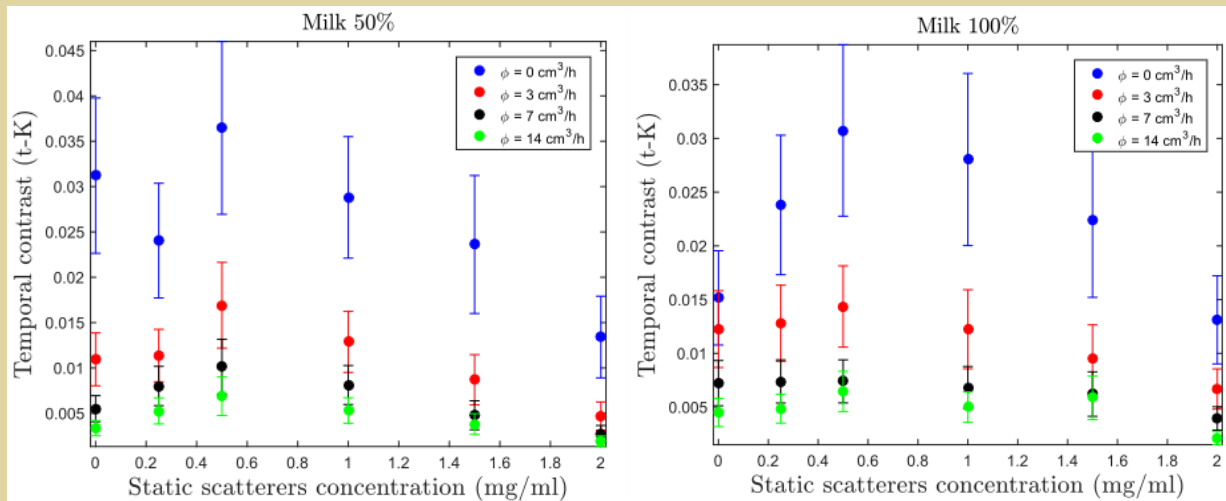
Speckle Contrast

Microcirculation results

The temporal contrast is less influenced by variations of the static scatterers.

It presents a strong variation only when the flow is zero.

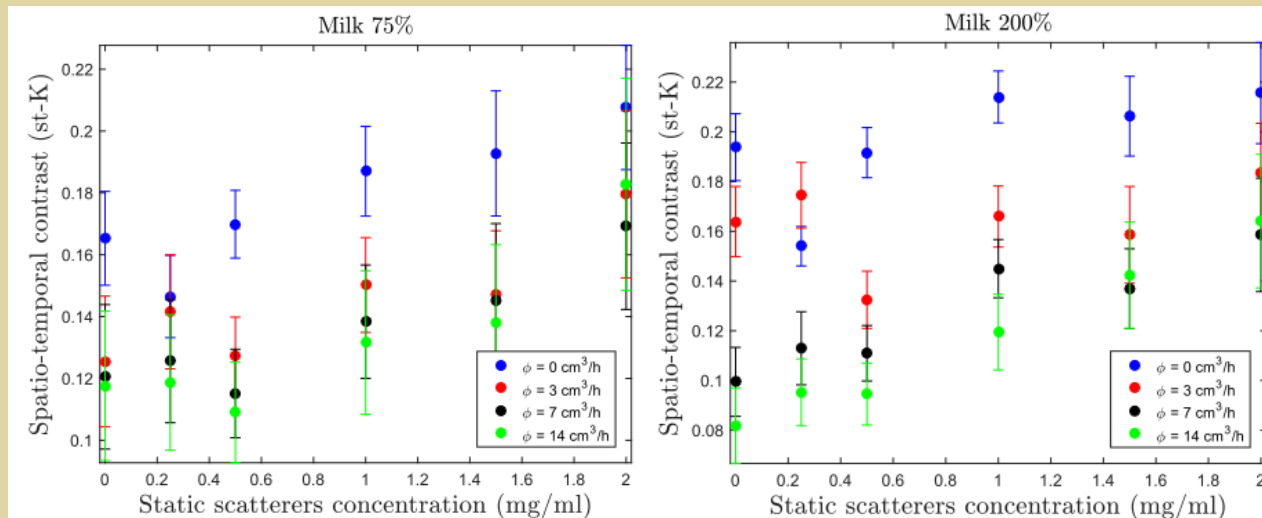
Its absolute values do not correspond to the spatial contrast values.



Speckle Contrast

Microcirculation results

The spatio-temporal contrast presents the best compromise between low static scatterers influence and good absolute values.



Remarks

Microcirculation results

This study proved that variations in the concentration of both dynamic and static scatterers cause alteration of the LSI data.

The fact that the speckle correlation is not sensitive to fluid flow variations can be considered as the main finding of this study. This characteristic is very important in order to validate speckle correlation as a metric to estimate the concentration of static and dynamic scatterers.

Spatial speckle is strongly influenced by the variations of the static scatterers concentration, highlighting the necessity of a different metric to account for this issue.

Temporal speckle behave better when static scatterers are present, however its absolute values do no agree with LSI theory.